

β -Secretase cleavage is not required for generation of the intracellular C-terminal domain of the amyloid precursor family of proteins

Carlo Sala Frigerio¹, Julia V. Fadeeva², Aedín M. Minogue¹, Martin Citron^{3,*}, Fred Van Leuven⁴, Matthias Staufenbiel⁵, Paolo Paganetti⁵, Dennis J. Selkoe² and Dominic M. Walsh¹

¹ Laboratory for Neurodegenerative Research, The Conway Institute for Biomolecular and Biomedical Research, University College Dublin, Republic of Ireland

² Department of Neurology, Harvard Medical School and Center for Neurologic Diseases, Brigham and Women's Hospital, Boston, MA, USA

³ Amgen Inc., Thousand Oaks, CA, USA

⁴ Department of Human Genetics, Katholieke Universiteit Leuven, Belgium

⁵ Nervous System Research, Novartis Institutes for Biomedical Research, Basel, Switzerland

Keywords

Alzheimer's disease; amyloid precursor protein (APP); amyloid precursor-like protein 1 (APLP1); amyloid precursor-like protein 2 (APLP2); β -site amyloid precursor protein-cleaving enzyme (BACE1)

Correspondence

Dominic M. Walsh, Laboratory for Neurodegenerative Research, The Conway Institute for Biomolecular and Biomedical Research, University College Dublin, Belfield, Dublin 4, Republic of Ireland
Fax: +353 1 716 6890
Tel: +353 1 7166751
E-mail: dominic.walsh@ucd.ie

*Present address

Eli Lilly and Company, Indianapolis, IN 46285, USA

(Received 31 October 2009, revised 6 January 2010, accepted 12 January 2010)

doi:10.1111/j.1742-4658.2010.07579.x

The amyloid precursor family of proteins are of considerable interest, both because of their role in Alzheimer's disease pathogenesis and because of their normal physiological functions. In mammals, the amyloid precursor protein (APP) has two homologs, amyloid precursor-like protein (APLP) 1 and APLP2. All three proteins undergo ectodomain shedding and regulated intramembrane proteolysis, and important functions have been attributed to the full-length proteins, shed ectodomains, C-terminal fragments and intracellular domains (ICDs). One of the proteases that is known to cleave APP and that is essential for generation of the amyloid β -protein is the β -site APP-cleaving enzyme 1 (BACE1). Here, we investigated the effects of genetic manipulation of BACE1 on the processing of the APP family of proteins. BACE1 expression regulated the levels and species of full-length APLP1, APP and APLP2, of their shed ectodomains, and of their membrane-bound C-terminal fragments. In particular, APP processing appears to be tightly regulated, with changes in β -cleaved APPs (APPs β) being compensated for by changes in α -cleaved APPs (APPs α). In contrast, the total levels of soluble cleaved APLP1 and APLP2 species were less tightly regulated, and fluctuated with BACE1 expression. Importantly, the production of ICDs for all three proteins was not decreased by loss of BACE1 activity. These results indicate that BACE1 is involved in regulating ectodomain shedding, maturation and trafficking of the APP family of proteins. Consequently, whereas inhibition of BACE1 is unlikely to adversely affect potential ICD-mediated signaling, it may alter other important facets of amyloid precursor-like protein/APP biology.

Abbreviations

A β , amyloid β -peptide; APLP, amyloid precursor-like protein; APLP1s, soluble C-terminally truncated form of amyloid precursor-like protein 1; APLP2s, soluble C-terminally truncated form of amyloid precursor-like protein 2; APP, amyloid precursor protein; APP_i, immature amyloid precursor protein; APP_m, mature amyloid precursor protein; APPs, soluble C-terminally truncated form of amyloid precursor protein; APPs α , soluble C-terminally truncated α -cleaved form of amyloid precursor protein; APPs β , soluble C-terminally truncated β -cleaved form of amyloid precursor protein; BACE1, β -site amyloid precursor protein-cleaving enzyme; CTF, C-terminal fragment; FLAPLP, full-length amyloid precursor-like protein; FLAPP, full-length amyloid precursor protein; GAPDH, glyceraldehyde-3-phosphate dehydrogenase; ICD, intracellular domain; ICDivg, intracellular domain *in vitro* generation; KO, knockout; Tg, transgenic.

Introduction

Genetic evidence indicates that the amyloid precursor protein (APP) is centrally involved in Alzheimer's disease pathogenesis [1], but it also appears to have important physiological functions. APP belongs to an evolutionarily conserved family of type I transmembrane glycoproteins [2], which includes the mammalian homologs amyloid precursor-like protein (APLP) 1 [3] and APLP2 [4]. These three proteins share a considerable degree of sequence and domain similarity [5,6]. Both APP and APLP2 are expressed in a variety of tissues and cell types [4,7], whereas APLP1 expression is neuron-specific [8]. The APP family of proteins is believed to play important roles in both the peripheral and central nervous systems [6]. In the former, they are involved in the formation and correct functioning of the neuromuscular junction [9], and in the latter they have been implicated in neurite outgrowth [10], synaptogenesis [11], and neuronal migration during embryogenesis [12]. Knockout (KO) studies indicate a high degree of functional redundancy between APP, APLP1 and APLP2 [13], with only subtle defects being observed in animals with ablation of one member [14]. In contrast, APP/APLP2 and APLP1/APLP2 double KO mice die soon after birth [14], and mice lacking all three proteins die *in utero* [13]. Surprisingly, APP/APLP1 double KO mice are viable and healthy, indicating that APLP2 possesses some functions that cannot be compensated for by APP and APLP1 [13].

There is also considerable evidence that the APP family of proteins have a role in cell-cell and cell-matrix adhesion, and that they can form both *cis* and *trans* homodimers and heterodimers [15,16]. In addition, the APP family of proteins can interact with a variety of cellular proteins that regulate APP, APLP1 and APLP2 processing. The majority of APP molecules are cleaved at the cell/luminal surface by α -secretase, resulting in the shedding of the ectodomain (soluble C-terminally truncated α -cleaved form of amyloid precursor protein, APPs α) [17,18]. α -Secretase cleavage is mediated by at least three enzymes, all of which are members of the ADAM (a disintegrin and metalloprotease) family [19]. A smaller fraction of APP molecules are proteolysed by β -secretase in endosomes or at the plasma membrane [20]. The β -secretase activity is attributed to a single protease, β -site APP-cleaving enzyme BACE1 [21,22]. BACE1 is an aspartyl protease and an atypical member of the pepsin family [21], and is also referred to as memapsin-2 [23] or Asp-2 [24]. The expression and activity of BACE1 are regulated at multiple levels [25], including mRNA transcription, mRNA stability, glycosylation,

proteolytic maturation, palmitoylation, and cellular localization.

Initial reports describing BACE1 KO mice failed to reveal significant defects [22,26]; however, recent studies have demonstrated that deletion of BACE1 results in impaired myelination [27,28] and in the development of behavioral abnormalities reminiscent of schizophrenia [29,30]. Both effects have been attributed to the loss of BACE1 cleavage of the neurotrophic factor neuregulin-1. In addition to APP and neuregulin-1, BACE1 has been shown to cleave type II α -2,6-sialyltransferase [31], P-selectin glycoprotein ligand-1 [32], the β 2-subunit of sodium channels [33] and interleukin-1 receptor type II [34]. However, loss of BACE1 processing of these latter substrates has not yet been shown to have significant adverse consequences.

Like APP, both APLP1 and APLP2 undergo ectodomain shedding, and their soluble ectodomains have been detected in the conditioned media of transfected cell lines and in human cerebrospinal fluid [35–37]. Although substantial data indicate that APLP2 is cleaved by both α -secretase and β -secretase [38,39], the enzymes involved in APLP1 ectodomain cleavage are less well defined [40,41]. Irrespective of the identity of the enzymes involved, ectodomain shedding of APP, APLP1 and APLP2 results in the generation of membrane-bound C-terminal fragments (CTFs). These CTFs are further processed by γ -secretase, releasing intracellular domains (ICDs) [42,43] that are postulated to be involved in transcriptional regulation [44,45]. Although the transcriptional properties of ICDs are contentious [45–48], there is consensus that the APP family of proteins may function as membrane anchors for a variety of proteins, and when CTFs are cleaved, ICDs, together with associated proteins, are released from the membrane [49].

Here we investigated the effects of genetic manipulation of BACE1 on the processing of APP, APLP1 and APLP2, and on the production of their ICDs. We report that BACE1 KO and overexpression affect the steady-state levels of full-length APLP (FLAPLP) 1 and FLAPLP2 similarly to the way in which they affect the steady-state levels of APP [50]. BACE1 expression also regulates the levels and species of the shed ectodomains and membrane-bound CTFs. In particular, APP processing appears to be tightly regulated, with the total levels of soluble APP remaining constant irrespective of the presence or absence of BACE1. The levels of APPs α increased to account for the loss of APPs β (soluble C-terminally truncated β -cleaved form of amyloid precursor protein) in BACE1 KO mice,

and decreased when APPs β levels increased because of BACE1 overexpression. In contrast, the total levels of soluble cleaved APLP1 and APLP2 species fluctuated with BACE1 expression. Importantly, we show that the production of ICDs for all three proteins is not decreased by a loss of BACE1 activity, indicating that BACE1 inhibition would not adversely affect ICD production.

Results

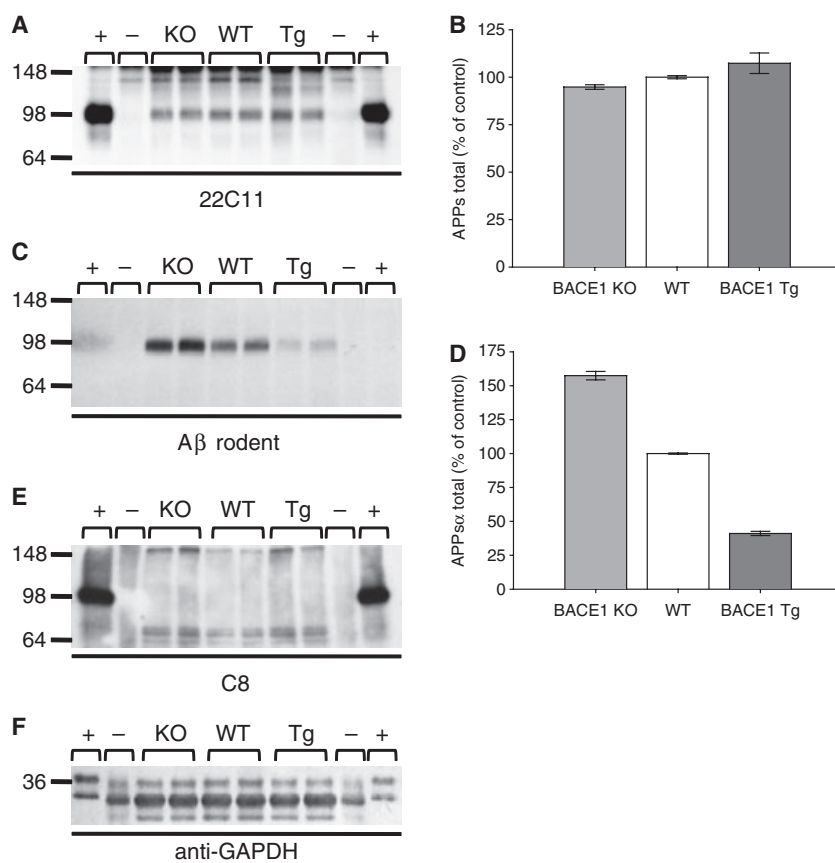
BACE1 regulates APP, APLP1 and APLP2 ectodomain shedding and secretion of FLAPLP1

Using murine models of BACE1 overexpression [BACE1 transgenic (Tg)] and deletion (BACE1 KO), we set out to investigate the role of BACE1 in the processing of APLP1 and APLP2. To do this, we employed an extraction procedure capable of separating water-soluble and membrane-associated proteins. First, water-soluble parenchymal and cytosolic proteins were extracted in NaCl/Tris, the membrane pellet was washed with sodium carbonate, and proteins were extracted using NaCl/Tris containing 1% Triton X-100 (NaCl/Tris-T). Secreted proteins were detected

using ectodomain-specific antibodies, and full-length proteins and CTFs were detected using antibodies that specifically recognize the C-termini of the different proteins. The specificity of antibodies for their cognate target proteins was confirmed using brains from APP, APLP1 and APLP2 KO mice (Fig. S1).

In NaCl/Tris extracts of mouse brains, 22C11, a monoclonal antibody recognizing an epitope between amino acids 66 and 81 of APP (Fig. S1), specifically detected a single band at around 100 kDa in wild-type (WT), BACE1 KO and BACE1 Tg samples that roughly comigrated with a strong band detected in lysates of human APP₆₉₅-expressing cells and that was absent in the APP KO sample (Fig. 1A). When the same samples were western blotted with C8, an antibody specifically recognizing an epitope at the extreme C-terminus of APP (Fig. S1), a \sim 100 kDa band was detected only in the lysate of APP₆₉₅-expressing cells (Fig. 1E). The fact that the \sim 100 kDa band detected in the NaCl/Tris mouse brain extracts was revealed by the ectodomain-directed antibody 22C11 but not by the C-terminal specific antibody C8 indicates that this protein lacks an intact C-terminus and probably represents secreted forms of APP (APPs). The levels of total APPs species were not significantly altered by either

Fig. 1. Levels of total APPs are unaffected by changes in BACE1 expression, whereas APPs α levels are dependent on BACE1 activity. NaCl/Tris homogenates of brains from WT, BACE1 KO and BACE1 Tg mice were electrophoresed on 10% Tris/glycine polyacrylamide gels and western blotted with a panel of antibodies that allow detection of total APPs [22C11 (A)], APPs α [anti- β rodent (C)] and full-length and C-terminal fragments of APP [C8 (E)]. Western blotting for GAPDH was included to check for equal protein loading (F). Lysates of a cell line overexpressing human WT APP₆₉₅ (+) were included as a positive control, and NaCl/Tris homogenates of brains from APP KO mice (–) were included as a negative control. The levels of total APPs and of APPs α [(B) and (D), respectively] were quantitated by densitometry, and values normalized versus WT control are presented as averages \pm standard errors of duplicate measurements of three animals of each genotype.



KO or overexpression of BACE1 (Fig. 1A,B). When the same samples were western blotted using a polyclonal antibody capable of detecting APPs α , but not APPs β (Fig. S1), a single band of ~ 100 kDa was detected in WT, BACE1 KO and BACE1 Tg mice, but was absent in both the APP KO mice and in the cell lysate sample (Fig. 1C). The lack of detection of full-length APP (FLAPP) in APP₆₉₅-expressing cells is due to the fact that the epitope for the antibody against rodent A β is not present in human APP (Table 1), whereas the absence of this band in the APP KO extract confirms the specificity of this band as a true APPs species (Fig. 1C). The levels of this APPs α band were dramatically increased in BACE1 KO mice (+57.4% \pm 3.1%, *P* < 0.0001) and decreased in BACE1 Tg mice (−58.9% \pm 1.6%, *P* < 0.0001) (Fig. 1C,D). Given that the total amounts of protein loaded for the different extracts were very similar (Fig. 1F), and that total APPs levels were unchanged (Fig. 1A,B), these results imply a tight regulation of APP ectodomain shedding, with overexpression of BACE1 causing a compensatory decrease in APPs α levels, and BACE1 ablation causing a compensatory increase in APPs α levels. These changes are unlikely to have resulted from a difference in genetic background, as a nearly identical pattern was seen when other BACE1 KO and BACE1 Tg mouse lines were examined (Fig. S3).

Western blot analysis of NaCl/Tris homogenates using W1NT, an antibody directed against the N-terminal domain of APLP1 (Fig. S1), revealed two specific bands in BACE1 KO, WT and BACE1 Tg samples that were not present in the APLP1 KO sample (Fig. 2A). The band migrating at ~ 94 kDa was present only in the BACE1 KO samples, and migrated just below the band from lysates of cells overexpressing human APLP1₆₅₀; an additional band, which migrated at ~ 83 kDa, was also present in WT and BACE1 KO samples (Fig. 2A). Moreover, when the same samples were analyzed by western blotting with

W1CT, a polyclonal antibody raised against the extreme C-terminus of APLP1 (Fig. S1), or a commercial antibody against the C-terminus of APLP1, 171615 (Calbiochem, EMD Biosciences, Merck KGaA, Darmstadt, Germany) (not shown), a band migrating at ~ 94 kDa was detected in all BACE1 KO, WT and BACE1 Tg samples, but not in APLP1 KO samples (Fig. 1C). As the band migrating at ~ 94 kDa was recognized by antibodies directed to both the ectodomain and the C-terminus, this band appears to be FLAP-PLP1. In contrast, the band migrating at ~ 83 kDa, which was recognized by W1NT and not by W1CT, is likely to be a soluble C-terminally truncated form of APLP1 (APLP1s). It is unusual for a transmembrane protein to be found in a detergent-free aqueous environment. One possible explanation for this behavior may be that FLAPPLP1 is present in membrane fractions, such as exosomes or microvesicles, that are not readily sedimented by centrifugation. Whatever the reason, the levels of APLP1s were dramatically reduced in BACE1 KO samples (−47.1% \pm 5.4%, *P* < 0.0001) and slightly increased by BACE1 overexpression (+11.4% \pm 4.1%, nonsignificant) (Fig. 2A,B). As W1NT cannot discriminate between APLP1s produced by α -secretase and that produced by β -secretase, we can only assess the effects on total APLP1s production. Accordingly, BACE1 seems to be required for the production of at least half of the total amount of APLP1s, as its deletion caused a ~ 50% decrease in APLP1s level (Fig. 2A). Given that overexpression of BACE1 did not lead to a significant increase in the levels of APLP1s (Fig. 2A,B), it would appear that APLP1s production is tightly regulated by factors other than BACE1 expression. A feature of APLP1, which is unique among the members of the APP family, is its secretion as unprocessed full-length protein (compare Figs 1E, 2C and 3C). Moreover, this property appears to be modulated by BACE1, as deletion of BACE1 caused a large increase in the levels of FLAPPLP1 released (+251% \pm 4.7%, *P* < 0.0001),

Table 1. Antibodies recognizing the APP family of proteins. Details about the specific target protein, epitope recognized, host, species specificities and source are provided for each antibody used. The amino acid numbering is for human sequences of APP₆₉₅, APLP1₆₅₀ and APLP2₇₅₁. For antibody against rodent A β , numbering is for the A β sequence. H, human; M, mouse.

Antibody	Target	Antigen, amino acid numbering	Host	Species reactivity	Source
22C11	APP	66–81	Mouse	H, M	Chemicon
Antibody against rodent A β	APP	3–16 A β	Rabbit	M	Signet
C8	APP	676–695	Rabbit	H, M	Selkoe laboratory
W1NT	APLP1	75–90	Rabbit	H, M	Walsh laboratory
W1CT	APLP1	640–650	Rabbit	H, M	Walsh laboratory
D2-II	APLP2	Full-length	Rabbit	H, M	Calbiochem
W2CT	APLP2	740–751	Rabbit	H, M	Walsh laboratory

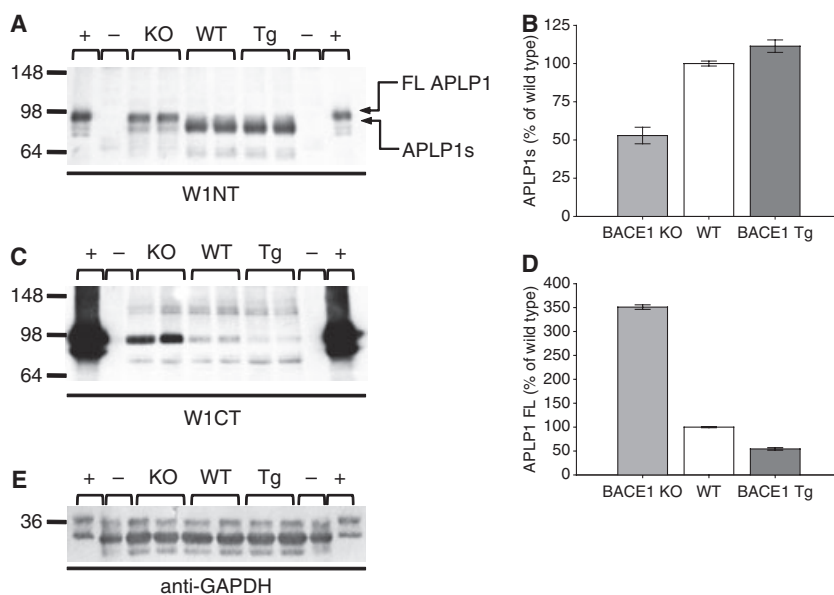


Fig. 2. BACE1 deletion decreases the levels of APLP1s and increases the levels of FLAPLP1. NaCl/Tris homogenates of brains from WT, BACE1 KO and BACE1 Tg mice were electrophoresed on 10% Tris/glycine polyacrylamide gels and western blotted with antibodies recognizing the N-terminus [W1NT (A)] and C-terminus [W1CT (C)] of APLP1. Western blotting for GAPDH was included to check for equal protein loading (E). Lysates of a cell line overexpressing human APLP1₆₅₀ (+) are included as a positive control, and NaCl/Tris homogenates of brains from APLP1 KO mice (-) are included as a negative control. FLAPLP1 and APLP1s bands detected by W1NT are indicated by arrows in (A). The levels of APLP1s and FLAPLP1 [(B) and (D), respectively] were quantitated by densitometry, and values normalized relative to WT control are presented as averages \pm standard errors of duplicate measurements of three animals of each genotype.

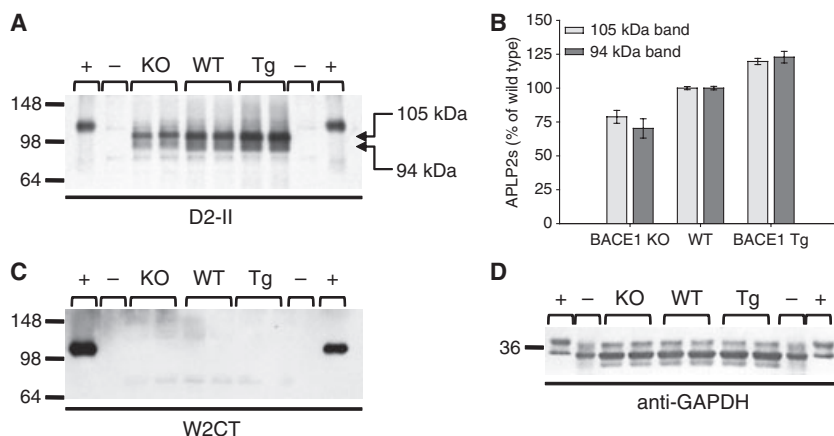


Fig. 3. BACE1 deletion decreases APLP2s levels, whereas BACE1 overexpression increases APLP2s levels. NaCl/Tris homogenates of brains from WT, BACE1 KO and BACE1 Tg mice were electrophoresed on 10% Tris/glycine polyacrylamide gels and western blotted with antibodies recognizing either FLAPLP2 [D2-II (A)] or the extreme C-terminus of APLP2 [W2CT (C)]. Western blotting for GAPDH was included to check for equal protein loading (D). Lysates of cell lines overexpressing human WT APLP2₇₅₁ (+) are included as a positive control, and NaCl/Tris homogenates of brains from APLP2 KO mice (-) are included as a negative control. APLP2s bands [indicated by arrows (A)] were quantitated by densitometry, and values normalized versus the WT control are presented as averages \pm standard errors of duplicate measurements of three animals of each genotype (B).

whereas BACE1 overexpression resulted in a sizeable reduction in FLAPLP1 release ($-45.6\% \pm 2.8\%$, $P < 0.0001$) (Fig. 2C,D). Thus expression of BACE1 regulates the release of FLAPLP1 and strongly influ-

ences the production of APLP1s. As with APP, these results are independent of genetic background, and have been replicated in other BACE1 KO and Tg mouse lines (Fig. S4).

Western blot analysis of NaCl/Tris homogenates using D2-II, an antibody raised against FLAPLP2 (Fig. S1), identified two bands migrating at ~ 105 and ~ 94 kDa in the WT, BACE1 KO and BACE1 Tg samples, but not in APLP2 KO samples (Fig. 3A). Both bands migrated considerably faster than the band detected in the lysate of human APLP2₇₅₁-expressing cells, which migrated at ~ 111 kDa (Fig. 3A). Western blot analysis with W2CT detected the ~ 111 kDa band in the lysates of APLP2₇₅₁-expressing cells, but did not detect any specific bands in NaCl/Tris extracts of mouse brain (Fig. 3C). Together, these data indicate that the ~ 94 and ~ 105 kDa bands detected by D2-II but not by W2CT probably represent soluble APLP2 (APLP2s). BACE1 deletion caused decreases in the levels of both APLP2s species (105 kDa, -21.2% ± 4.8%, *P* < 0.0001; 94 kDa, -29.8% ± 7.1%, *P* < 0.0001), whereas BACE1 overexpression caused increases (105 kDa, +19.7% ± 2.3%, *P* < 0.0005; 94 kDa, +22.8% ± 4.3%, *P* < 0.005) (Fig. 3A,B). As with APP and APLP1, these results were independent of genetic background (Fig. S5), and indicate that BACE1 is responsible for the generation of at least ~ 20% of APLP2s.

BACE1 manipulation alters the quantity and form of APP, APLP1 and APLP2 CTFs

To examine the effects of BACE1 expression on full-length proteins and CTFs, membrane fractions of

mouse brains were analyzed using C-terminus-specific antibodies. Analysis using the APP-specific C8 antibody revealed the presence of two high molecular mass bands in WT, BACE1 KO and BACE1 Tg mice, but not in APP KO samples (Fig. 4A). These two bands, which comigrated with similar bands detected in the lysate of APP₆₉₅-expressing cells, most probably represent mature (APP_m; ~ 96 kDa) and immature (APP_i; ~ 91 kDa) forms of APP (Fig. 4A) [51,52]. The levels of both forms were significantly increased by BACE1 deletion (APP_m, +48.4% ± 3.1%, *P* < 0.0001; APP_i, +35.4% ± 3.3%, *P* < 0.0001) and significantly decreased by BACE1 overexpression (APP_m, -45.5% ± 1.4%, *P* < 0.0001; APP_i, -26.7% ± 1.0%, *P* < 0.0001) (Fig. 4B). These differences did not result from changes in the expression of APP, as APP mRNA levels were unchanged in brains of genetically modified animals (Fig. S6A). Although effects on both forms of FLAPP followed the same trend, the ratio of ~ 96 to ~ 91 kDa FLAPP was increased in BACE1 KO samples (1.31 ± 0.05 versus 1.19 ± 0.02, *P* < 0.01) and decreased in BACE1 Tg samples (0.89 ± 0.02 versus 1.19 ± 0.02, *P* < 0.0001). These results imply that BACE1 expression influences the levels of FLAPP by a mechanism independent of direct proteolysis.

Analysis with C8 also revealed a series of low molecular mass species of sizes consistent with CTFs (Fig. 4C). Two CTFs of approximately 13.3 and 12.5 kDa were detected in WT and BACE1 KO sam-

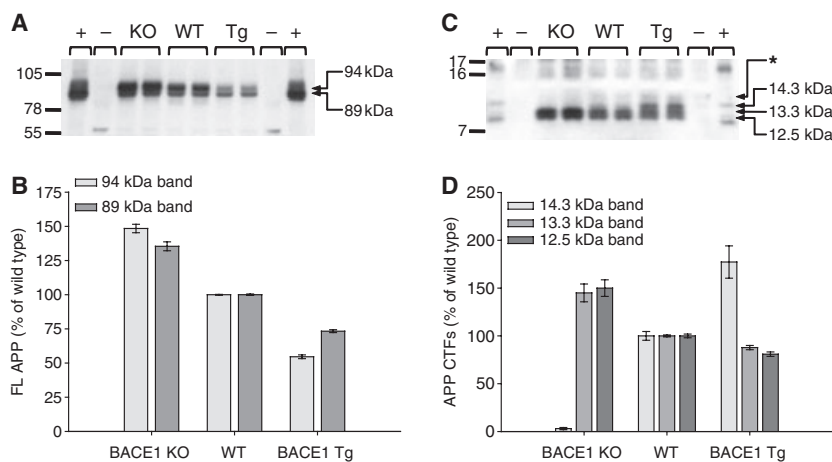


Fig. 4. BACE1 expression decreases FLAPP steady-state levels and gives rise to a ~ 14.3 kDa APP CTF. NaCl/Tris-T homogenates of WT, BACE1 KO and BACE1 Tg mouse brains were electrophoresed on 10–20% Tris/Tricine polyacrylamide gels and western blotted with specific antibody against the APP C-terminus [C8, (A, C)]. Lysates of a cell line overexpressing human WT APP₆₉₅ (+) are included as a positive control, and NaCl/Tris-T homogenates of brains from APP KO mice (-) are included as a negative control. The asterisk in (C) indicates a specific band detected in certain WT and Tg samples. Full-length and CTF bands [indicated by arrows in (A) and (C), respectively] were quantified by densitometry and normalized versus the WT control (B, D). Results are presented as averages ± standard errors of duplicate measurements of three animals for each condition.

ples (Fig. 4C), and the levels of both were increased in the latter (13.3 kDa, $+45.0\% \pm 9.3\%$, $P < 0.0001$; 12.5 kDa, $+50.0\% \pm 8.7\%$, $P < 0.0001$). In contrast, the levels of both the ~ 13.3 and ~ 12.5 kDa bands were slightly decreased in BACE1 Tg samples (13.3 kDa, $-12.2\% \pm 2.2\%$, nonsignificant; 12.5 kDa, $-19.1\% \pm 2.3\%$, $P < 0.05$), and a third CTF band migrating at around 14.3 kDa was detected (Fig. 4C). A faint ~ 14.3 kDa band was also detected in WT samples (BACE1 Tg $+77.3\% \pm 16.9\%$ versus wild type, $P < 0.0001$) but was not present in BACE1 KO samples. These results indicated that the ~ 14.3 kDa band is a BACE1 cleavage product (Fig. 4D). An additional faint band migrating at ~ 15.4 kDa (indicated by an asterisk in Fig. 4C) was occasionally detected in WT and BACE1 Tg mice only. In other experiments using different lines of BACE1 KO and BACE1 Tg mice, the changes in FLAPP and APP CTFs were very similar to those reported above (Fig. S3). In all of the mouse lines studied, the total amounts of CTFs were not altered by BACE1 expression, a finding in keeping with the fact that the levels of total APPs are not altered by BACE1 expression, and which suggests that the change in FLAPP is not the result of a net change in APP processing or APP expression (Fig. S6) but is mediated by a BACE1-regulated change in turnover or trafficking.

Western blot analysis of NaCl/Tris-T homogenates with antibody W1CT revealed two discrete bands, migrating at ~ 88 and ~ 80 kDa in WT, BACE1 KO

and BACE1 Tg mice, that were absent in APLP1 KO samples (Fig. 5A). As revealed by N-glycosidase F treatment, the slower-migrating specific band is N-glycosylated APLP1 (Fig. S7); therefore, by analogy with FLAPP (Fig. 4A), these two bands may represent mature and immature APLP1 (Fig. 5A) [37]. Following the trend seen for APP (Fig. 4B), the slower-migrating FLAPLP1 band was dramatically increased ($+92.2\% \pm 4.6\%$, $P < 0.0001$) in the BACE1 KO samples and decreased in the BACE1 Tg samples ($-19.2\% \pm 2.4\%$, $P < 0.0005$) (Fig. 5B). On the other hand, the ~ 80 kDa APLP1 band was decreased in the BACE1 KO samples ($-65.2\% \pm 3.0\%$, $P < 0.0001$) and unchanged in the BACE1 Tg samples ($-0.5\% \pm 7.0\%$, nonsignificant) (Fig. 5B). As was the case for FLAPP, the differences seen in the levels of FLAPLP1 are not due to a difference in the levels of APLP1 mRNA (Fig. S6B). Importantly, the ratio of mature to immature FLAPLP1 was drastically shifted towards the mature form in BACE1 KO samples (15.28 ± 1.04 versus 2.78 ± 0.29 , $P < 0.0001$) and was unchanged in the BACE1 Tg samples (2.31 ± 0.33 versus 2.78 ± 0.29), suggesting that BACE1 may regulate the maturation of APLP1. For WT, BACE1 KO and BACE1 Tg samples, a single CTF band was detected, the size of which varied with BACE1 expression (Fig. 5C). In BACE1-deficient mice, this band migrated at ~ 8.2 kDa, whereas in samples from WT and BACE1 Tg mice, it migrated at ~ 7.8 kDa. These data indicate that deletion of BACE1

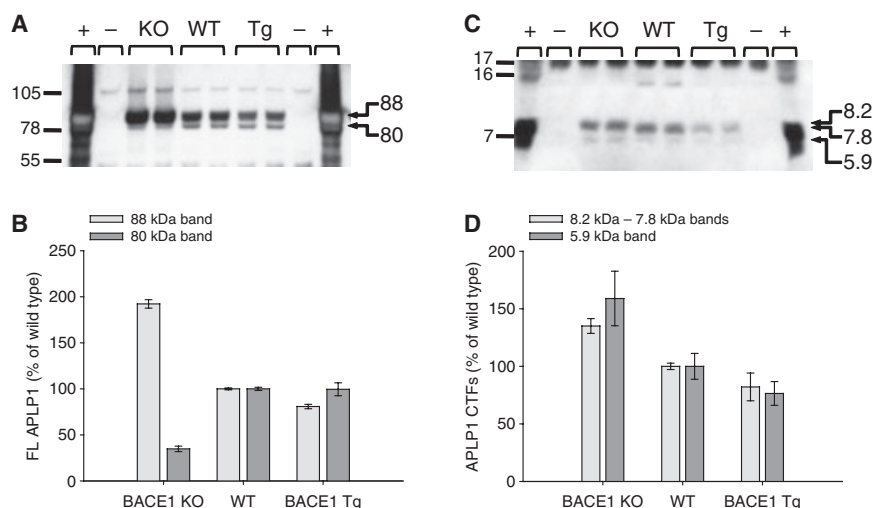


Fig. 5. BACE1 expression decreases FLAPLP1 levels and gives rise to a ~ 7.5 kDa APLP1 CTF. NaCl/Tris-T homogenates of WT, BACE1 KO and BACE1 Tg mouse brains were electrophoresed on 10–20% Tris/Tricine polyacrylamide gels and western blotted with specific antibody against the APLP1 C-terminus [W1CT (A, C)]. Lysates of a cell line overexpressing human WT APLP1₆₅₀ (+) are included as a positive control, and NaCl/Tris-T homogenates of brains from APLP1 KO mice (–) are included as a negative control. The full-length and CTF species identified [indicated by arrows in (A) and (C), respectively] were quantified by densitometry and normalized versus the WT control, and results are presented as averages \pm standard errors of duplicate measurements of three animals for each condition [(B) FLAPLP1; (D) APLP1 CTF].

precludes the production of normal APLP1 CTF, leading to the production of a slightly longer CTF (Fig. 5C). The effective differences in the molecular masses of APLP1 CTFs from BACE1 KO mice and from WT and BACE1 Tg mice were confirmed by using a 12-cm-long 16% polyacrylamide Tris/Tricine gel, and, in these gels, two tightly migrating bands were detected (not shown). This suggests that two distinct APLP1s forms can be produced, although the relative molecular weights would be too close to be effectively separated on a 10% Tris/glycine gel (Fig. 2A). Thus it would appear that BACE1 is the principal sheddase for APLP1, and that only when BACE1 activity is deleted can APLP1 be cleaved by another activity. It is also of note that the amount of APLP1 CTF in BACE1 KO samples tended to be greater than in the wild type ($+35.1\% \pm 6.4\%$, $P < 0.0005$), whereas APLP1 CTF was slightly decreased in BACE1 Tg samples ($-17.9\% \pm 12.0\%$, nonsignificant) (Fig. 5D). A second very faint CTF band migrating around 5.9 kDa was seen in all samples, and its levels were slightly elevated in BACE1 KO samples ($+59.0\% \pm 23.7\%$, $P < 0.005$) and slightly lower in BACE1 Tg samples ($-23.6\% \pm 10.3\%$, nonsignificant) (Fig. 5D). However, whether this band represents an authentic CTF or a membrane-associated ICD is unclear (see below for more details). As with APP, the effects of BACE1 expression were replicated in a distinct set of mouse lines (Fig. S4).

Analysis of NaCl/Tris-T samples with W2CT (Fig. 6A,C) revealed a broad ~ 92 kDa band (which, on occasion, appeared as a doublet) in WT, BACE1 KO and BACE1 Tg samples (Fig. 6A). The difference in molecular mass observed for FLAPLP2 from mouse brains and from transfected CHO cells probably reflects the presence of different APLP2 isoforms and/or differences in post-translational modifications. The levels of the ~ 92 kDa FLAPLP2 were increased in BACE1 KO samples ($+39.4\% \pm 2.3\%$, $P < 0.0001$) and decreased in BACE1 Tg samples ($-27.4\% \pm 0.9\%$, $P < 0.0001$) (Fig. 6B). As was the case also for FLAPP and FLAPLP1, differences in FLAPLP2 are not the result of differential expression of APLP2 mRNA (Fig. S6C).

APLP2 processing generates at least four CTFs: three higher molecular mass bands migrating close together at ~ 14.8 kDa, ~ 13.4 and ~ 12.6 kDa, respectively, and a fourth lower molecular mass band migrating at ~ 9.6 kDa (Fig. 6C). Because of the close migration of APLP2 CTFs, quantitative densitometric analysis of each species was not possible. However, the ~ 14.8 and ~ 9.6 kDa bands were quantified separately, and the ~ 13.4 and ~ 12.6 kDa bands were considered together. The ~ 14.8 kDa APLP2 CTF is probably the product of BACE1 cleavage, as this band was absent in BACE1 KO samples and was increased in BACE1 Tg samples ($+80.3\% \pm 11.6\%$, $P < 0.0001$) (Fig. 6D). The ~ 9.6 kDa APLP2 CTF was found in all samples,

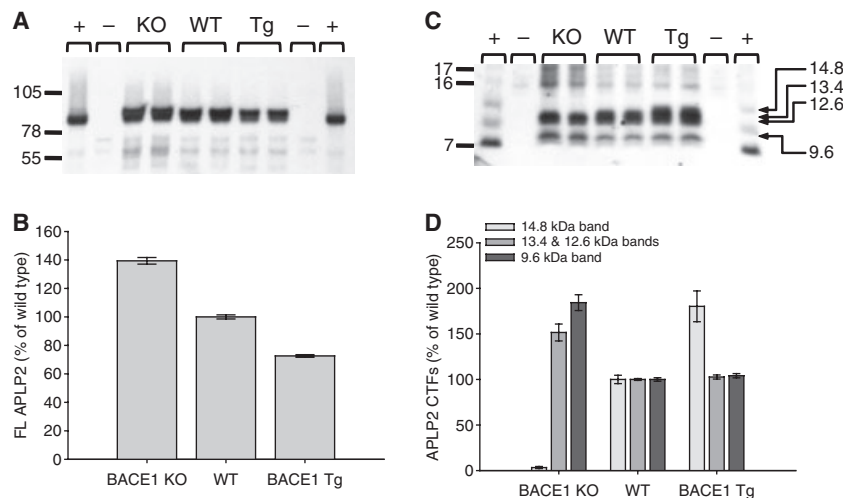


Fig. 6. BACE1 expression decreases FLAPLP2 protein levels and gives rise to a ~ 14.8 kDa APLP2 CTF. NaCl/Tris-T homogenates of WT, BACE1 KO and BACE1 Tg mouse brains were electrophoresed on 10–20% Tris/Tricine polyacrylamide gels and western blotted with specific antibody against the APLP2 C-terminus [W2CT (A, C)]. Lysates of a cell line overexpressing human WT APLP2₇₅₁ (+) are included as a positive control, and NaCl/Tris-T homogenates of hemibrains of APLP2 KO mice (–) are included as a negative control. The full-length and CTF species identified [indicated by arrows in (A) and (C), respectively] were quantified by densitometry and normalized versus the WT control. Results are presented as averages \pm standard errors of duplicate measurements of three animals for each condition [(B) FLAPLP2; (D) APLP2 CTF].

being increased by an average of $84.3\% \pm 17.6\%$ ($P < 0.0001$) in BACE1 KO samples and unchanged in BACE1 Tg samples (Fig. 6D). The ~ 13.4 and ~ 12.6 kDa bands were essentially unchanged in BACE1 Tg samples and increased in BACE1 KO samples (Fig. 6D). With regard to total CTF levels, BACE1 deletion led to a minor increase, whereas BACE1 over-expression caused a significant increase. The increase in total CTF levels in BACE1 Tg samples are in keeping with the increase in total APLP2s level (Fig. 3B), whereas this is not the case for BACE1 KO, where we observed a substantial decrease in APLP2s level (Fig. 3A,B) and a minor increase in total APLP2 CTF level (Fig. 6D). However, there is a good correspondence between the levels of APLP2s and FLAPLP2, with the level of FLAPLP2 being increased and that of APLP2s being decreased in BACE1 KO samples. The same trends for APLP2s, FLAPLP2 and APLP2 CTFs were confirmed in mice of a different genetic background (Fig. S5). Taken together, these data suggest that BACE1 expression largely mediates regulation of APLP2 by direct proteolysis.

BACE1 deletion does not impair ICD production

As CTFs are the direct precursors of ICD generation, and as BACE1 expression alters the size of CTFs, we investigated whether or not BACE1 cleavage was

necessary for ICD production. This was accomplished by searching for endogenous ICDs in mouse brain and by the use of an *in vitro* ICD generation (ICDivg) assay. For all three proteins, a single band migrating at ~ 5.8 kDa was produced by microsomes from both BACE1 KO and WT mice (Fig. 7A–C). When the ICDivg assay was performed in the presence of protease inhibitors, we found an increase in the total amount of ICD produced (Fig. 7A–C). This finding is in keeping with prior reports that ICDs produced from the APP family of proteins are degraded by insulin-degrading enzyme [43,53], and hence are stabilized in the presence of insulin-degrading enzyme inhibitors. The levels of ICDs tended to be higher in samples from BACE1 KO brains than in those from WT brains (Fig. 7A–C). Therefore, the deletion of BACE1, and consequently the loss of BACE1 processing of APP, APLP1 and APLP2, had no detrimental effect on the *de novo* production of ICDs (compare lanes 2 and 3 and lanes 1 and 4 in Fig. 7A–C).

In a complementary approach, we also sought to determine whether the physiological production of ICDs was altered by BACE1 deletion. As ICDs are extremely labile [53,54], mouse brains were processed in a fashion designed to minimize ICD degradation, and the ICDs present in the homogenates were analyzed by immunoprecipitation and western blotting using antibodies C8, W1CT and W2CT. A ladder of bands was detected migrating until the 7 kDa marker

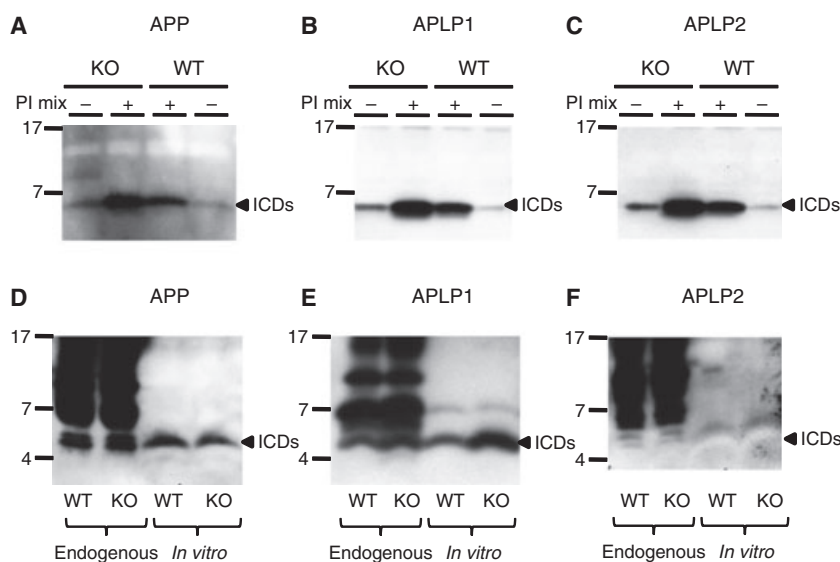


Fig. 7. BACE1 deletion does not compromise APP, APLP1 and APLP2 ICD generation. Microsomes prepared from BACE1 KO or WT mouse brains were incubated at 37 °C for 2 h to allow *de novo in vitro* ICD production (A–C). ICDs were detected by western blot using specific antibodies against APP [C8 (A)], APLP1 [W1CT (B)] and APLP2 [W2CT (C)]. Western blots shown in (A)–(C) are representative of three different experiments. Generation of ICDs was conducted either in the presence (+) or in the absence (–) of protease inhibitors and insulin (PI mix). Endogenous ICDs were immunoprecipitated from mouse brains with C8, W1CT or W2CT, and immunoprecipitates were analyzed by western blotting with the same antibodies (D–F). The western blots shown in (D)–(F) are representative of two different experiments. For comparison, *in vitro*-generated ICDs were electrophoresed alongside endogenous ICDs (D–F).

in all immunoprecipitates (Fig. 7D–F). These bands probably represent various CTFs, consistent with previous reports [54], and nonspecific bands due to the use of the same polyclonal antibody for both immunoprecipitation and western blotting. In addition, less abundant lower molecular mass bands were detected. For APP, two closely migrating bands with estimated molecular masses of ~ 5.8 and ~ 6.4 kDa were detected (Fig. 7D). The lower of the two bands perfectly comigrated with *in vitro*-generated APP ICDs, with the upper band migrating in a manner consistent for phosphorylated APP ICD [55]. Moreover, as with the brain microsome-generated APP ICDs, these two bands were slightly more abundant in the BACE1 KO samples (Fig. 7D), a result that we observed in two separate experiments using a total of two BACE1 KO and two WT mouse brains. For APLP1, a similar ladder of bands was detected, together with a single putative ICD band that comigrated with *in vitro*-generated APLP1 ICD (Fig. 7E). Again, the levels of the endogenous APLP1 ICD were slightly higher in extracts of BACE1 KO brains. For APLP2, the pattern was similar to that for APP, i.e. a putative ICD band that comigrated with *in vitro*-generated APLP2 ICD at ~ 5.8 kDa, together with a slightly slower-migrating band at ~ 6.4 kDa (Fig. 7F).

Discussion

By analogy with APP, both APLP1 and APLP2 have been proposed to be substrates of BACE1 [41]. Moreover, a previous study found evidence that APLP2 is cleaved by BACE1 *in vivo* [38], but the processing of APLP1 and APLP2 by BACE1 has so far been mainly studied in transfected cell lines [40,41]. As trafficking and interaction with other cellular partners are likely to be altered when a single member of the APP family of proteins is overexpressed [56], we set out to investigate the effects of BACE1 on APLP1 and APLP2 in mouse models where the only variable parameter was expression of BACE1.

All three APP family proteins underwent ectodomain shedding, and their soluble ectodomains were detected in the NaCl/Tris fraction of brain homogenates (for a summary of results, see Table S2). Shedding of the APP ectodomain appears to be tightly regulated, as BACE1 levels altered the ratio of APP α to APP β , but did not substantially modify the total levels of APPs or of APP CTFs. This suggests that there is a discrete pool of FLAPP that is directed towards processing, and that α -secretases and β -secretases have access to the same cellular pool. For APLP1, ablation of BACE1 resulted in a near complete loss of APLP1s,

suggesting that BACE1 is centrally involved in APLP1 ectodomain cleavage, a notion supported by the finding that the FLAPLP1 level is increased by deletion of BACE1 and slightly decreased by BACE1 overexpression. However, the current data cannot discriminate between cleavage of APLP1 by BACE1 and cleavage of APLP1 by another enzyme regulated by BACE1. Indeed, prior studies using cell culture systems have found APLP1 to be cleaved by an α -secretase-like activity [40,57]. Importantly, BACE1 overexpression did not dramatically alter APLP1 processing (as assessed by APLP1s and APLP1 CTF levels), suggesting that the ectodomain shedding of APLP1, although not as tightly regulated as APP, is nonetheless closely regulated.

Interestingly, FLAPLP1 was detected in the NaCl/Tris brain homogenates, an observation consistent with the detection of FLAPLP1 in conditioned media from transfected cells [43]. Moreover, the levels of secreted FLAPLP1 were influenced by BACE1 expression, mirroring the modifications of the levels of FLAPLP1 in the NaCl/Tris-T fraction. An attractive explanation for the presence of FLAPLP1 in NaCl/Tris homogenates is its secretion via vesicles, e.g. exosomes [58]. Indeed, it is interesting to note that the prion protein, which is known to interact with APLP1 [59] and to be a regulator of BACE1 activity [60], can be secreted via exosomes [59]. Whatever the mechanism for secretion of FLAPLP1, the net outcome of these results suggests that BACE1 has a key role in the regulation of APLP1 maturation, trafficking and secretion.

BACE1 expression also regulates the steady-state levels of FLAPLP2, in a manner analogous to what has been shown for APP [50] and to what has been presented here for APLP1. As BACE1 did not alter the levels of APP, APLP1 and APLP2 mRNA, it would appear that BACE1 is an important post-transcriptional regulator of the APP family of proteins. In agreement with previous reports [38,50], we detected β -cleavage-specific products for both APP and APLP2. In addition, we detected a slightly longer APLP1 CTF when BACE1 was deleted, but we did not see an effect of BACE1 overexpression on the size of this CTF. We also found that the total amounts of APP and APLP2 CTFs were not altered by BACE1 expression, meaning that competing or complementary pathways intervene to balance the loss of BACE1 cleavage. In direct NaCl/Tris-T extracts, we could not detect ICDs of either APP or APLP2, but we did detect a band consistent with APLP1 ICD, possibly because APLP1 ICDs are more stable than either APP or APLP2 ICDs [43,53,54].

This characterization of BACE1 effects on APP, APLP1 and APLP2 has highlighted the fact that APP and APLP2 share many similarities, whereas APLP1

has some unique characteristics. APLP1 is an atypical member of the APP family: it is neuron-specific, whereas APP and APLP2 are ubiquitously expressed, and its subcellular localization and dimerization properties are different from those of APP and APLP2 [16]. Given the similarities between processing of Notch and of the APP family of proteins, it seems plausible that APP, APLP1 and APLP2 ICDs could play a role in transcriptional regulation [42,43]. The APP ICD has been shown to form a complex with the adaptor protein Fe65 and the histone acetyltransferase Tip60 that is capable of inducing transcription of reporter genes [44]. The ability to form transcriptionally active complexes with Fe65 has also been demonstrated for APLP ICDs [42,43]; however, definite physiological relevance of these complexes has yet to be demonstrated.

As we found that BACE1 activity regulates the maturation and the processing of the three APP family members, we were interested determining whether abolishing BACE1 activity had a detrimental effect on APP, APLP1 and APLP2 ICD production, to better characterize the impact of BACE1 inhibition as a putative therapy for the treatment of AD. We found that the *de novo* production and the endogenous levels of ICDs were not reduced by deletion of BACE1. In fact, in most cases, deletion of BACE1 resulted in an increase in the levels of ICDs. Indeed, treatment of cultured cells with a potent β -secretase inhibitor (Fig. S8) consistently resulted in a slight elevation of ICD production. However, how genetic or chemical ablation of BACE1 leads to a modest increase in ICD levels is unclear. One potential explanation is that, owing to spatial differences, α -secretase-derived CTFs are more prone to γ -secretase cleavage than β -secretase-derived CTFs. The fact that BACE1 deletion does not dramatically alter ICD production opens two possible scenarios: one where ICDs produced by γ -secretase cleavage of α -secretase-derived and β -secretase-derived CTFs serve the same function and their levels are tightly regulated by compensatory mechanisms, and another where only ICDs produced by α -secretase cleavage are physiologically relevant, and ICDs derived from the amyloidogenic processing of APP are quickly degraded. This latter possibility is corroborated by the fact that overexpression of BACE1, while leading to increased processing of APP and APLP2, does not translate into increased amounts of APP or APLP2 CTFs. Therefore, it is reasonable to suppose that the levels of CTFs are regulated, possibly by degradation of excess CTFs.

Together, these results demonstrate that BACE1 is involved in ectodomain shedding of APP, APLP1 and APLP2. BACE1 expression levels appear to regulate the trafficking and maturation of the APP family of

proteins, but BACE1 ablation did not prevent generation of APP, APLP1 and APLP2 ICDs. This suggests that inhibition of BACE1 will not adversely affect the potentially important signaling role of the ICDs released by the APP family of proteins, but may impact on other functions of this family of proteins.

Experimental procedures

Reagents

Unless otherwise specified, chemicals were from Sigma-Aldrich (Sigma-Aldrich Ireland Ltd, Dublin, Ireland).

Antibodies

Novel rabbit polyclonal antibodies W1NT, W1CT and W2CT were raised against peptide immunogens conjugated to keyhole limpet hemocyanin via an N-terminal cysteine (Table 1). W1NT was raised against residues EPDPQR SRRCLRDPQR of the human APLP1 ectodomain, and W1CT and W2CT were raised against peptides NPTYR-FLEERP and NPTYKYLEQMQL, corresponding to the extreme C-termini of human APLP1 and human APLP2, respectively (Fig. S1A). The sequences against which W1CT and W2CT were raised are identical in both human and mouse proteins. The sequence against which W1NT was raised differs in one of the 16 amino acids from the corresponding murine region (R12K, antigen numbering); as expected, W1NT recognizes both murine and human APLP1 (Table 1). The specificity of antibodies W1NT, W1CT and W2CT was confirmed by western blotting of brain material from mice null for APP, APLP1 or APLP2 (Fig. S1B). The monoclonal antibody 22C11 (Chemicon, Millipore, Billerica, MA, USA), which recognizes the N-terminus of APP, the polyclonal antiserum C8, which recognizes the C-terminus of APP, and the polyclonal antiserum D2-II, which recognizes the ectodomain of APLP2 (Calbiochem, EMD Chemicals Inc., Gibbstown, NJ, USA), have been described previously [43] (Table 1). The polyclonal antibody against the BACE1 N-terminus was from Sigma (Dublin, Ireland), and the polyclonal antibody against rodent amyloid β -peptide ($A\beta$) was from Signet (Signet Covance, Dedham, MA, USA). The monoclonal antibody against glyceraldehyde-3-phosphate dehydrogenase (GAPDH) was from Abcam (Cambridge, UK).

Animals

All genetically manipulated mouse lines have been described previously [26,38,50,61]. Black Swiss BACE1 KO and littermate control WT mouse brains and C57/BL6 BACE1 Tg mouse brains were from 4-month-old mice. Additional mouse brains from C57/BL6-OLA129 BACE2

KO mice, C57/B6Jx129SVola BACE1 KO mice, C57/BL6 WT mice and C57/BL6 BACE1 Tg mice were from 4-month-old mice. Immediately after explant, the cerebellum and olfactory bulb were removed, and the remaining brain was cut in half along the midline, snap frozen in liquid nitrogen, and stored at -80°C until analysis. Levels of BACE1 protein in all of the brain tissues analyzed were assessed by western blotting (Fig. S2). Brains from APP, APLP1 and APLP2 KO mice were provided by U. Müller (University of Heidelberg, Heidelberg, Germany) [14].

Animal care and handling were performed according to the Declaration of Helsinki and approved by local ethical committees.

Preparation of mouse brain extracts

Hemibrains were homogenized in five volumes of NaCl/Tris (20 mM Tris, pH 7.4, 150 mM NaCl) containing protease inhibitors (5 mM EDTA, 1 mM EGTA, $5\ \mu\text{g}\cdot\text{mL}^{-1}$ leupeptin, $5\ \mu\text{g}\cdot\text{mL}^{-1}$ aprotinin, $2\ \mu\text{g}\cdot\text{mL}^{-1}$ pepstatin, $120\ \mu\text{g}\cdot\text{mL}^{-1}$ Pefabloc, 2 mM 1,10-phenanthroline) with 40 strokes of a Dounce homogenizer at 5000 r.p.m. The resulting suspension was then centrifuged at 175 000 *g* and 4°C for 30 min, and the upper 75% of the supernatant was collected. Protein content was assessed using a bicinchoninic acid protein assay kit (Pierce, Rockford, IL, USA), and samples were then aliquoted and stored at -80°C until use. The membrane-containing pellet was resuspended by pipetting in five volumes of 100 mM sodium bicarbonate (pH 11.4), and incubated on a rocking platform for 15 min at 4°C . The washed pellet was harvested by centrifugation, as described above and washed in five volumes of NaCl/Tris. The membrane fraction was again pelleted by centrifugation as described above, and then resuspended by pipetting in five volumes of NaCl/Tris-T plus protease inhibitors. In order to ensure effective extraction of integral membrane proteins, this suspension was incubated on a rocking platform at room temperature for 15 min, homogenized with 40 strokes of a Dounce homogenizer, and sonicated with a microtip attached to an XL-2000 sonicator (Misonix Inc., Farmingdale, NY, USA) at power setting 4 ($\sim 12\ \text{W}$) for 30 s. The detergent extract was centrifuged as described above, and the upper 75% of the supernatant was collected. Protein content was assessed using a bicinchoninic acid protein assay kit (Pierce), and samples were then aliquoted and stored at -80°C until use.

Quantitative real-time PCR analysis

Total RNA was isolated using TRI Reagent (Ambion, Austin, TX, USA) according to the manufacturer's instructions, and quantified using a Nanodrop spectrophotometer (Thermo Scientific, Wilmington, DE, USA). One-microgram aliquots of total RNA were treated with deoxyribonuclease I (Invitrogen, Carlsbad, CA, USA) and used to synthesize first-strand cDNA with 200 U of SuperScript II Reverse

Transcriptase (Invitrogen) in a final reaction volume of 11 μL , containing 50 ng of random hexamers. One microliter of the first-strand cDNA PCR reaction was used as template for quantitative real-time PCR amplification with primers specific for APP, APLP1 and APLP2 (Sigma-Genosys, Hamburg, Germany) (Table S1). Primers specific for the 18S rRNA were used as an internal control. Primer pairs for the APP family of proteins contained one intron-spanning region to avoid amplification of genomic DNA. Quantitative real-time PCR reactions were run in duplicate. One microliter of *Taq* DNA polymerase and the appropriate primer pair, each at a concentration of 0.5 μM , together with the Power SYBR Green PCR Master Mix (Invitrogen), were brought to a final volume of 10 μL and analyzed on an ABI Prism 7000 Sequence Detection System (Applied Biosystems, Darmstadt, Germany). An initial step of 15 min at 95°C for polymerase activation was followed by 40 cycles of a standard PCR protocol (15 s at 95°C , 30 s at 60°C , 30 s at 72°C) as described in the supplier's protocol (Applied Biosystems). APP, APLP1 and APLP2 expression was normalized to 18S rRNA levels by the comparative cycle threshold (Ct) method.

ICDivg assay with mouse brain-derived microsomes

This method was adapted from an ICD *in vitro* generation assay previously used with microsomes prepared from cultured cells [62]. Hemibrains were homogenized on ice in eight volumes of hypotonic lysis buffer (10 mM Mops, pH 7, containing 10 mM KCl, 5 mM EDTA, 1 mM EGTA, $120\ \mu\text{g}\cdot\text{mL}^{-1}$ Pefabloc, and 2 mM 1,10-phenanthroline) with 30 passes of a Dounce homogenizer at 6000 r.p.m. The resulting homogenate was divided into 1 mL aliquots, and centrifuged at 1000 *g* and 4°C for 15 min, the supernatant was then transferred to a new tube, and microsomes were harvested by centrifugation at 16 000 *g* and 4°C for 40 min. Each pellet derived from 1 mL of homogenate was resuspended in 100 μL of assay buffer (150 mM sodium citrate, pH 6.8) either containing or devoid of a cocktail of protease inhibitors (5 mM EDTA, 1 mM EGTA, 2 mM 1,10-phenanthroline, $250\ \mu\text{g}\cdot\text{mL}^{-1}$ human recombinant insulin). Microsomes were then incubated in a water bath at 37°C for 2 h, after which they were placed on ice for 10 min to stop the reaction, and centrifuged at 150 000 *g* and 4°C for 75 min in an Optima centrifuge, using a TLA55 rotor (Beckman Coulter, Fullerton, CA, USA). The upper 90 μL of the supernatant was collected for analysis by western blotting.

Immunoprecipitation of endogenous ICDs from mouse brains

Hemibrains were homogenized on ice in nine volumes of homogenization buffer (50 mM Tris/HCl, pH 7.4, containing

1% SDS, 150 mM NaCl, 5 mM EDTA, 5 $\mu\text{g}\cdot\text{mL}^{-1}$ leupeptin, 5 $\mu\text{g}\cdot\text{mL}^{-1}$ aprotinin, 2 $\mu\text{g}\cdot\text{mL}^{-1}$ pepstatin, 120 $\mu\text{g}\cdot\text{mL}^{-1}$ Pefabloc, 2 mM 1,10-phenanthroline) with 30 passes of a Dounce homogenizer at 6000 r.p.m. The homogenates were then boiled at 100 °C for 10 min, and divided into 1 mL aliquots prior to sonication for 30 s at power setting 4 (~12 W), using a XL-2000 sonicator connected to a microtip (Misonix Inc.). Following sonication, aliquots were pooled, boiled for a further 10 min, and then centrifuged at 16 000 *g* for 20 min. The supernatant was collected, transferred to a fresh tube, and diluted 1 : 10 with lysis buffer (50 mM Tris base, pH 7.6, containing 150 mM NaCl, 5 mM EDTA, 2% NP-40, 5 $\mu\text{g}\cdot\text{mL}^{-1}$ leupeptin, 5 $\mu\text{g}\cdot\text{mL}^{-1}$ aprotinin, 2 $\mu\text{g}\cdot\text{mL}^{-1}$ pepstatin, 120 $\mu\text{g}\cdot\text{mL}^{-1}$ Pefabloc, and 2 mM 1,10-phenanthroline). To immunoprecipitate APP, APLP1 and APLP2 ICDs, 1 mL aliquots of brain extracts were incubated overnight on a rocking platform at 4 °C with either antibody C8, W1CT or W2CT, respectively (at a dilution of 1 : 40), together with 40 μL of protein A-Sepharose. Beads were collected by centrifugation at 6000 *g* for 5 min, and washed in subsequent steps of incubation for 20 min on a rocking platform at 4 °C with 0.5 M STEN buffer (50 mM Tris base, pH 7.6, 500 mM NaCl, 2 mM EDTA, 2% NP-40), SDS/STEN buffer (50 mM Tris base, pH 7.6, 150 mM NaCl, 2 mM EDTA, 2% NP-40, 0.1% SDS) and STEN buffer (50 mM Tris base, pH 7.6, 150 mM NaCl, 2 mM EDTA, 2% NP-40). Captured proteins were eluted with 2 \times Tris/Tricine electrophoresis sample buffer containing 10% β -mercaptoethanol (20 μL per sample) [63].

Western blot analysis

NaCl/Tris homogenates of mouse brains were diluted with 4 \times Tris/glycine sample buffer ($\times 1$ concentrations: 62.5 mM Tris/HCl, pH 6.8, 10% glycerol, 2% SDS) and electrophoresed on 10% polyacrylamide Tris/glycine gels [64], and NaCl/Tris-T homogenates of mouse brains and ICDivg samples were diluted with 4 \times Tris/Tricine sample buffer ($\times 1$ concentrations: 450 mM Tris, pH 8.45, 10% glycerol, 4% SDS) and electrophoresed on precast Novex 10–20% polyacrylamide Tris/Tricine gels (Invitrogen). Immunoprecipitated endogenous ICDs from mouse brains were also electrophoresed on precast Novex 10–20% polyacrylamide Tris/Tricine gels (Invitrogen). Proteins were transferred onto nitrocellulose (0.2 μm pore size; Sigma-Aldrich Ltd) at 400 mA and 4 °C for 2 h. Membranes were subsequently blocked for 1 h at room temperature with 5% skimmed milk (Fluka, Sigma-Aldrich Ireland Ltd) in NaCl/Tris-Tw, washed twice for 10 min with NaCl/Tris-Tw to remove traces of blocker, and incubated overnight with primary antibodies diluted in NaCl/Tris-Tw containing 5% skimmed milk. On the following day, blots were washed four times for 15 min with NaCl/Tris-Tw, incubated with appropriate horseradish peroxidase-

linked secondary antibodies (Amersham, GE Healthcare, Chalfont St Giles, UK) for 1 h at room temperature, washed as above, and visualized using an enhanced chemiluminescence kit (Pierce) and Hyperfilm MP (Amersham, GE Healthcare).

Data analysis

Band intensities were quantified using SCION IMAGE (Scion Corporation, Frederick, MD, USA), and data were analyzed using one-way ANOVA (SIGMASTAT; Systat Software Inc., Chicago, IL, USA).

Acknowledgements

The authors thank U. Müller (University of Heidelberg, Heidelberg, Germany) for APP, APLP1 and APLP2 KO mouse brains, J. Tang (Protein Studies Program, Oklahoma Medical Research Foundation, University of Oklahoma Health Science Center, Oklahoma City, OK 73104, USA) for the β -secretase inhibitor GRL-8234, B. Boland (UCD, Dublin, Ireland) for help with the midi Tris/Tricine PAGE gels, and T. Young-Pearse (CND, Harvard Medical School, Boston, USA) for constructive discussions and critical reading of the manuscript. This work was supported by Wellcome Trust grant 067660 (D. M. Walsh), NIH grant AG027443 (D. M. Walsh and D. J. Selkoe), and the Foundation for Neurologic Diseases (D. M. Walsh).

References

- Selkoe DJ (2001) Alzheimer's disease: genes, proteins, and therapy. *Physiol Rev* **81**, 741–766.
- Coulson EJ, Paliga K, Beyreuther K & Masters CL (2000) What the evolution of the amyloid protein precursor supergene family tells us about its function. *Neurochem Int* **36**, 175–184.
- Wasco W, Bupp K, Magendantz M, Gusella JF, Tanzi RE & Solomon F (1992) Identification of a mouse brain cDNA that encodes a protein related to the Alzheimer disease-associated amyloid beta protein precursor. *Proc Natl Acad Sci USA* **89**, 10758–10762.
- Wasco W, Gurubhagavatula S, Paradis MD, Romano DM, Sisodia SS, Hyman BT, Neve RL & Tanzi RE (1993) Isolation and characterization of APLP2 encoding a homologue of the Alzheimer's associated amyloid beta protein precursor. *Nat Genet* **5**, 95–100.
- Bayer TA, Wirths O, Majtenyi K, Hartmann T, Multhaup G, Beyreuther K & Czech C (2001) Key factors in Alzheimer's disease: beta-amyloid precursor protein processing, metabolism and intraneuronal transport. *Brain Pathol* **11**, 1–11.

- 6 Walsh DM, Minogue AM, Sala Frigerio C, Fadeeva JV, Wasco W & Selkoe DJ (2007) The APP family of proteins: similarities and differences. *Biochem Soc Trans* **35**, 416–420.
- 7 Schmechel DE, Goldgaber D, Burkhardt DS, Gilbert JR, Gajdusek DC & Roses AD (1988) Cellular localization of messenger RNA encoding amyloid-beta-protein in normal tissue and in Alzheimer disease. *Alzheimer Dis Assoc Disord* **2**, 96–111.
- 8 Kim TW, Wu K, Xu JL, McAuliffe G, Tanzi RE, Wasco W & Black IB (1995) Selective localization of amyloid precursor-like protein 1 in the cerebral cortex postsynaptic density. *Brain Res Mol Brain Res* **32**, 36–44.
- 9 Wang P, Yang G, Mosier DR, Chang P, Zaidi T, Gong YD, Zhao NM, Dominguez B, Lee KF, Gan WB *et al.* (2005) Defective neuromuscular synapses in mice lacking amyloid precursor protein (APP) and APP-like protein 2. *J Neurosci* **25**, 1219–1225.
- 10 Small DH, Nurcombe V, Reed G, Clarris H, Moir R, Beyreuther K & Masters CL (1994) A heparin-binding domain in the amyloid protein precursor of Alzheimer's disease is involved in the regulation of neurite outgrowth. *J Neurosci* **14**, 2117–2127.
- 11 Priller C, Bauer T, Mitteregger G, Krebs B, Kretschmar HA & Herms J (2006) Synapse formation and function is modulated by the amyloid precursor protein. *J Neurosci* **26**, 7212–7221.
- 12 Young-Pearse TL, Bai J, Chang R, Zheng JB, LoTurco JJ & Selkoe DJ (2007) A critical function for beta-amyloid precursor protein in neuronal migration revealed by in utero RNA interference. *J Neurosci* **27**, 14459–14469.
- 13 Herms J, Anliker B, Heber S, Ring S, Fuhrmann M, Kretschmar H, Sisodia S & Muller U (2004) Cortical dysplasia resembling human type 2 lissencephaly in mice lacking all three APP family members. *EMBO J* **23**, 4106–4115.
- 14 Heber S, Herms J, Gajic V, Hainfellner J, Aguzzi A, Rulicke T, von Kretschmar H, von Koch C, Sisodia S, Tremml P *et al.* (2000) Mice with combined gene knock-outs reveal essential and partially redundant functions of amyloid precursor protein family members. *J Neurosci* **20**, 7951–7963.
- 15 Soba P, Eggert S, Wagner K, Zentgraf H, Siehl K, Kreger S, Lower A, Langer A, Merdes G, Paro R *et al.* (2005) Homo- and heterodimerization of APP family members promotes intercellular adhesion. *EMBO J* **24**, 3624–3634.
- 16 Kaden D, Voigt P, Munter LM, Bobowski KD, Schaefer M & Multhaup G (2009) Subcellular localization and dimerization of APLP1 are strikingly different from APP and APLP2. *J Cell Sci* **122**, 368–377.
- 17 Esch FS, Keim PS, Beattie EC, Blacher RW, Culwell AR, Oltersdorf T, McClure D & Ward PJ (1990) Cleavage of amyloid beta peptide during constitutive processing of its precursor. *Science* **248**, 1122–1124.
- 18 Sisodia SS (1992) Beta-amyloid precursor protein cleavage by a membrane-bound protease. *Proc Natl Acad Sci USA* **89**, 6075–6079.
- 19 Allinson TM, Parkin ET, Turner AJ & Hooper NM (2003) ADAMs family members as amyloid precursor protein alpha-secretases. *J Neurosci Res* **74**, 342–352.
- 20 Koo EH & Squazzo SL (1994) Evidence that production and release of amyloid beta-protein involves the endocytic pathway. *J Biol Chem* **269**, 17386–17389.
- 21 Vassar R, Bennett BD, Babu-Khan S, Kahn S, Mendiaz EA, Denis P, Teplow DB, Ross S, Amarante P, Loeloff R *et al.* (1999) Beta-secretase cleavage of Alzheimer's amyloid precursor protein by the transmembrane aspartic protease BACE. *Science* **286**, 735–741.
- 22 Cai H, Wang Y, McCarthy D, Wen H, Borchelt DR, Price DL & Wong PC (2001) BACE1 is the major beta-secretase for generation of Abeta peptides by neurons. *Nat Neurosci* **4**, 233–234.
- 23 Lin X, Koelsch G, Wu S, Downs D, Dashti A & Tang J (2000) Human aspartic protease memapsin 2 cleaves the beta-secretase site of beta-amyloid precursor protein. *Proc Natl Acad Sci USA* **97**, 1456–1460.
- 24 Hussain I, Powell D, Howlett DR, Tew DG, Meek TD, Chapman C, Gloger IS, Murphy KE, Southan CD, Ryan DM *et al.* (1999) Identification of a novel aspartic protease (Asp 2) as beta-secretase. *Mol Cell Neurosci* **14**, 419–427.
- 25 Willem M, Lammich S & Haass C (2009) Function, regulation and therapeutic properties of beta-secretase (BACE1). *Semin Cell Dev Biol* **20**, 175–182.
- 26 Luo Y, Bolon B, Kahn S, Bennett BD, Babu-Khan S, Denis P, Fan W, Kha H, Zhang J, Gong Y *et al.* (2001) Mice deficient in BACE1, the Alzheimer's beta-secretase, have normal phenotype and abolished beta-amyloid generation. *Nat Neurosci* **4**, 231–232.
- 27 Willem M, Garratt AN, Novak B, Citron M, Kaufmann S, Rittger A, DeStrooper B, Saftig P, Birchmeier C & Haass C (2006) Control of peripheral nerve myelination by the beta-secretase BACE1. *Science* **314**, 664–666.
- 28 Hu X, Hicks CW, He W, Wong P, Macklin WB, Trapp BD & Yan R (2006) Bace1 modulates myelination in the central and peripheral nervous system. *Nat Neurosci* **9**, 1520–1525.
- 29 Harrison SM, Harper AJ, Hawkins J, Duddy G, Grau E, Pugh PL, Winter PH, Shilliam CS, Hughes ZA, Dawson LA *et al.* (2003) BACE1 (beta-secretase) transgenic and knockout mice: identification of neurochemical deficits and behavioral changes. *Mol Cell Neurosci* **24**, 646–655.
- 30 Savonenko AV, Melnikova T, Laird FM, Stewart KA, Price DL & Wong PC (2008) Alteration of BACE1-

- dependent NRG1/ErbB4 signaling and schizophrenia-like phenotypes in BACE1-null mice. *Proc Natl Acad Sci USA* **105**, 5585–5590.
- 31 Kitazume S, Tachida Y, Oka R, Shirotani K, Saido TC & Hashimoto Y (2001) Alzheimer's beta-secretase, beta-site amyloid precursor protein-cleaving enzyme, is responsible for cleavage secretion of a Golgi-resident sialyltransferase. *Proc Natl Acad Sci USA* **98**, 13554–13559.
- 32 Lichtenthaler SF, Dominguez DI, Westmeyer GG, Reiss K, Haass C, Saftig P, De Strooper B & Seed B (2003) The cell adhesion protein P-selectin glycoprotein ligand-1 is a substrate for the aspartyl protease BACE1. *J Biol Chem* **278**, 48713–48719.
- 33 Kim DY, Carey BW, Wang H, Ingano LA, Binshtok AM, Wertz MH, Pettingell WH, He P, Lee VM, Woolf CJ *et al.* (2007) BACE1 regulates voltage-gated sodium channels and neuronal activity. *Nat Cell Biol* **9**, 755–764.
- 34 Kuhn PH, Marjaux E, Imhof A, De Strooper B, Haass C & Lichtenthaler SF (2007) Regulated intramembrane proteolysis of the interleukin-1 receptor II by alpha-, beta-, and gamma-secretase. *J Biol Chem* **282**, 11982–11995.
- 35 Slunt HH, Thinakaran G, Von Koch C, Lo AC, Tanzi RE & Sisodia SS (1994) Expression of a ubiquitous, cross-reactive homologue of the mouse beta-amyloid precursor protein (APP). *J Biol Chem* **269**, 2637–2644.
- 36 Webster MT, Groome N, Francis PT, Pearce BR, Sherriff FE, Thinakaran G, Felsenstein KM, Wasco W, Tanzi RE & Bowen DM (1995) A novel protein, amyloid precursor-like protein 2, is present in human brain, cerebrospinal fluid and conditioned media. *Biochem J* **310**, 95–99.
- 37 Paliga K, Peraus G, Kreger S, Durrwang U, Hesse L, Multhaup G, Masters CL, Beyreuther K & Weidemann A (1997) Human amyloid precursor-like protein 1 – cDNA cloning, ectopic expression in COS-7 cells and identification of soluble forms in the cerebrospinal fluid. *Eur J Biochem* **250**, 354–363.
- 38 Pastorino L, Ikin AF, Lamprianou S, Vacaresse N, Revelli JP, Platt K, Paganetti P, Mathews PM, Harroch S & Buxbaum JD (2004) BACE (beta-secretase) modulates the processing of APLP2 in vivo. *Mol Cell Neurosci* **25**, 642–649.
- 39 Endres K, Postina R, Schroeder A, Mueller U & Fahrenholz F (2005) Shedding of the amyloid precursor protein-like protein APLP2 by disintegrin-metalloproteinases. *FEBS J* **272**, 5808–5820.
- 40 Eggert S, Paliga K, Soba P, Evin G, Masters CL, Weidemann A & Beyreuther K (2004) The proteolytic processing of the amyloid precursor protein gene family members APLP-1 and APLP-2 involves alpha-, beta-, gamma-, and epsilon-like cleavages: modulation of APLP-1 processing by n-glycosylation. *J Biol Chem* **279**, 18146–18156.
- 41 Li Q & Sudhof TC (2004) Cleavage of amyloid-beta precursor protein and amyloid-beta precursor-like protein by BACE 1. *J Biol Chem* **279**, 10542–10550.
- 42 Scheinfeld MH, Ghersi E, Laky K, Fowlkes BJ & D'Adamio L (2002) Processing of beta-amyloid precursor-like protein-1 and -2 by gamma-secretase regulates transcription. *J Biol Chem* **277**, 44195–44201.
- 43 Walsh DM, Fadeeva JV, LaVoie MJ, Paliga K, Eggert S, Kimberly WT, Wasco W & Selkoe DJ (2003) gamma-Secretase cleavage and binding to FE65 regulate the nuclear translocation of the intracellular C-terminal domain (ICD) of the APP family of proteins. *Biochemistry* **42**, 6664–6673.
- 44 Cao X & Sudhof TC (2001) A transcriptionally [correction of transcriptively] active complex of APP with Fe65 and histone acetyltransferase Tip60. *Science* **293**, 115–120.
- 45 Scheinfeld MH, Matsuda S & D'Adamio L (2003) JNK-interacting protein-1 promotes transcription of A beta protein precursor but not A beta precursor-like proteins, mechanistically different than Fe65. *Proc Natl Acad Sci USA* **100**, 1729–1734.
- 46 Pardossi-Piquard R, Petit A, Kawarai T, Sunyach C, Alves da Costa C, Vincent B, Ring S, D'Adamio L, Shen J, Muller U *et al.* (2005) Presenilin-dependent transcriptional control of the Abeta-degrading enzyme neprilysin by intracellular domains of betaAPP and APLP. *Neuron* **46**, 541–554.
- 47 Hebert SS, Serneels L, Tolia A, Craessaerts K, Derks C, Filippov MA, Muller U & De Strooper B (2006) Regulated intramembrane proteolysis of amyloid precursor protein and regulation of expression of putative target genes. *EMBO Rep* **7**, 739–745.
- 48 Chen AC & Selkoe DJ (2007) Response to: Pardossi-Piquard *et al.*, 'Presenilin-dependent transcriptional control of the Abeta-degrading enzyme neprilysin by intracellular domains of betaAPP and APLP.' *Neuron* **53**, 479–483.
- 49 Bruni P, Minopoli G, Brancaccio T, Napolitano M, Faraonio R, Zambrano N, Hansen U & Russo T (2002) Fe65, a ligand of the Alzheimer's beta-amyloid precursor protein, blocks cell cycle progression by down-regulating thymidylate synthase expression. *J Biol Chem* **277**, 35481–35488.
- 50 Bodendorf U, Danner S, Fischer F, Stefani M, Sturchler-Pierrat C, Wiederhold KH, Staufenbiel M & Paganetti P (2002) Expression of human beta-secretase in the mouse brain increases the steady-state level of beta-amyloid. *J Neurochem* **80**, 799–806.
- 51 Weidemann A, Konig G, Bunke D, Fischer P, Salbaum JM, Masters CL & Beyreuther K (1989) Identification, biogenesis, and localization of precursors of Alzheimer's disease A4 amyloid protein. *Cell* **57**, 115–126.

- 52 Weidemann A, Eggert S, Reinhard FB, Vogel M, Paliga K, Baier G, Masters CL, Beyreuther K & Evin G (2002) A novel epsilon-cleavage within the transmembrane domain of the Alzheimer amyloid precursor protein demonstrates homology with Notch processing. *Biochemistry* **41**, 2825–2835.
- 53 Edbauer D, Willem M, Lammich S, Steiner H & Haass C (2002) Insulin-degrading enzyme rapidly removes the beta-amyloid precursor protein intracellular domain (AICD). *J Biol Chem* **277**, 13389–13393.
- 54 Kimberly WT, Zheng JB, Town T, Flavell RA & Selkoe DJ (2005) Physiological regulation of the beta-amyloid precursor protein signaling domain by c-Jun N-terminal kinase JNK3 during neuronal differentiation. *J Neurosci* **25**, 5533–5543.
- 55 Suzuki T & Nakaya T (2008) Regulation of APP by phosphorylation and protein interactions. *J Biol Chem* **283**, 29633–29637.
- 56 Neumann S, Schobel S, Jager S, Trautwein A, Haass C, Pietrzik CU & Lichtenthaler SF (2006) Amyloid precursor-like protein 1 influences endocytosis and proteolytic processing of the amyloid precursor protein. *J Biol Chem* **281**, 7583–7594.
- 57 Minogue AM, Stubbs AK, Frigerio CS, Boland B, Fadeeva JV, Tang J, Selkoe DJ & Walsh DM (2009) gamma-Secretase processing of APLP1 leads to the production of a p3-like peptide that does not aggregate and is not toxic to neurons. *Brain Res* **1262**, 89–99.
- 58 van Niel G, Porto-Carreiro I, Simoes S & Raposo G (2006) Exosomes: a common pathway for a specialized function. *J Biochem* **140**, 13–21.
- 59 Yehiely F, Bamorough P, Da Costa M, Perry BJ, Thinakaran G, Cohen FE, Carlson GA & Prusiner SB (1997) Identification of candidate proteins binding to prion protein. *Neurobiol Dis* **3**, 339–355.
- 60 Parkin ET, Watt NT, Hussain I, Eckman EA, Eckman CB, Manson JC, Baybutt HN, Turner AJ & Hooper NM (2007) Cellular prion protein regulates beta-secretase cleavage of the Alzheimer's amyloid precursor protein. *Proc Natl Acad Sci USA* **104**, 11062–11067.
- 61 Willem M, Dewachter I, Smyth N, Van Dooren T, Borghgraef P, Haass C & Van Leuven F (2004) beta-Site amyloid precursor protein cleaving enzyme 1 increases amyloid deposition in brain parenchyma but reduces cerebrovascular amyloid angiopathy in aging BACE \times APP[V717I] double-transgenic mice. *Am J Pathol* **165**, 1621–1631.
- 62 Sala Frigerio C, Kukar TL, Fauq A, Engel PC, Golde TE & Walsh DM (2009) An NSAID-like compound, FT-9, preferentially inhibits gamma-secretase cleavage of the amyloid precursor protein compared to its effect on amyloid precursor-like protein 1. *Biochemistry* **48**, 10894–10904.
- 63 Kimberly WT, Zheng JB, Guenette SY & Selkoe DJ (2001) The intracellular domain of the beta-amyloid precursor protein is stabilized by Fe65 and translocates to the nucleus in a notch-like manner. *J Biol Chem* **276**, 40288–40292.
- 64 Laemmli UK (1970) Cleavage of structural proteins during the assembly of the head of bacteriophage T4. *Nature* **227**, 680–685.

Supporting information

The following supplementary material is available:

Fig. S1. Antibodies recognizing the APP family of proteins.

Fig. S2. Confirmation of BACE1 overexpression and KO by immunoblotting using an antibody against BACE1.

Fig. S3. Effects of BACE1 expression on APP processing are independent of genetic background.

Fig. S4. Effects of BACE1 expression on APLP1 processing are independent of genetic background.

Fig. S5. Effect of BACE1 expression on APLP2 processing are independent of genetic background.

Fig. S6. APP, APLP1 and APLP2 mRNA levels are not altered by either deletion or overexpression of BACE1.

Fig. S7. The 94 kDa APLP1 species present in NaCl/Tris-T mouse brain homogenates is N-glycosylated.

Fig. S8. BACE1 inhibition slightly increases ICD production in differentiated N2a cells.

Table S1. Primers used for quantitative real-time analysis.

Table S2. Effects of BACE1 deletion and overexpression on APP, APLP1 and APLP2.

This supplementary material can be found in the online version of this article.

Please note: As a service to our authors and readers, this journal provides supporting information supplied by the authors. Such materials are peer-reviewed and may be re-organized for online delivery, but are not copy-edited or typeset. Technical support issues arising from supporting information (other than missing files) should be addressed to the authors.